Nationwide Cross-sectional and Seasonal Multicenter Study of Dermatological Patients in Japan

Masutaka Furue[1) 2)*], Souji Yamazaki[1)], Koichi Jimbow[1)],
Tetsuya Tsuchida[1)], Masayuki Amagai[1)], Toshihiro Tanaka[1) 2)],
Kayoko Matsunaga[1) 2)], Masahiko Muto[1) 2)], Eishin Morita[1) 2)],
Masashi Akiyama[2)], Yoshinao Soma[2)], Tadashi Terui[2)] and Motomu Manabe[2)]
[1)]Scientific Committee, Japanese Dermatological Association (2006-2007) (* : Chair)
[2)]Scientific Committee, Japanese Dermatological Association (2008-2009) (* : Chair)

[Purpose] To clarify incidence and difference of gender and age in skin disorders of dermatological patients in the early 21st century in Japan.

[Methods] Nationwide cross-sectional and seasonal multicenter study was conducted by 76 university hospitals, 55 district-based pivotal hospitals and 59 private clinics (190 clinics in total). In each clinic, information on diagnosis, age and gender was collected from all of the out-patients and in-patients visited on any one day of the second week of May, August and November 2007 and February 2008. Average high and low monthly temperature and humidity reports were collected from the Meteorological Agency.

[Results] The information on 67,448 cases from 170 clinics (69 university hospitals, 45 district-based pivotal hospitals and 56 private clinics) participated in all of the 4 seasonal examination, was analyzed. Top 20 skin disorders were, in high incidence order, miscellaneous eczema, atopic dermatitis, tinea pedis, urticaria/angioedema, tinea unguium, viral warts, psoriasis, contact dermatitis, acne, seborrheic dermatitis, hand eczema, miscellaneous benign skin tumors, alopecia areata, herpes zoster/postherpetic neuralgia, skin ulcers (non-diabetic), prurigo, epidermoid cysts, vitiligo vulgaris, sebborheic keratosis, and drug eruption/toxicoderma. The vast majority (85.34%) of dermatological patients were covered under the top 20 disorders. Each disorder showed its own specific age distribution. The number of patients was correlated with average high and low monthly temperature in disorders such as atopic dermatitis, contact dermatitis, urticaria/angioedema, prurigo, insect bites and tinea pedis. Male-prone (psoriasis, erythroderma, diabetic dermatoses, e. t. c.) and female-prone (erythema nodosum, collagen diseases, livedo reticularis/racemosa, hand eczema, e. t. c.) diseases were clearly evident.

[Conclusion] This study apparently highlights the present situation of dermatological patients in the early 21st century of Japan. It is necessary to continue to perform the similar study periodically from social dermatological point of view.

(Jpn J Dermatol 119: 1795～1809, 2009)
Key words: Dermatological patients, Diagnosis, Age, Gender

日皮会誌：119（13），2550—2553，2009（平21）

EL6—2　母斑症・色素性乾皮症

結節性硬化症のガイドライン

金田　眞理

はじめに

Tuberous sclerosis complex（結節性硬化症，TSC）は，1835にPFO Rayerによる顔面の血管線維腫（Facial angiofibroma）の報告にはじまる古くから知られた疾患で，その遺伝性に関しても1935年にすでにGuntherとPenroseにより常染色体優性遺伝と報告されていた[1]．しかしながら，その後50年以上にわたって殆ど進歩が認められなかった．1993年にEuropian chromosome 16 tuberous sclerosis consortiumによって16番の染色体上にTSCの遺伝子の一つ*TSC2*遺伝子[2]が，1997にvan Slegtenhorstらによって9番の染色体上に*TSC1*遺伝子[3]が相次いで同定され，本症の解明が飛躍的に進んだ．本症は全身の過誤腫を特徴とし，古典的には知能低下，癲癇発作及び顔面の血管線維腫を三主徴としてきたが，軽症例の増加に伴って，必ずしもこれら三主張の頻度は高くなく，むしろ最近では予後を左右する肺病変や腎病変に注目が集まってきている．

これらの変化をうけて，本邦では2002年に神経皮膚症候群研究班（厚生労働省科学研究費補助金・難治性疾患克服研究事業）からTSCを含む母斑症の治療指針，ガイドラインが提案された．さらに，2008年には日本皮膚科学会による結節性硬化症の診断基準及び治療指針が作成された[4]ので，それに基づいて最近のTSCの特徴，症状，診断及び治療方針について解説させて頂く．

TSCの最近の知見

2003年から2008年の5年間に阪大皮膚科でフォローされたTSC患者131人のうち，種々の検査が施行されている患者100名について，痙攣発作，精神発達遅滞，皮膚症状，肺症状　腎症状の頻度について検討した．その結果，精神発達遅滞や自閉症がある人は46%，痙攣発作のある人60%とそれぞれの従来の頻度60～70%，80%前後より遙かに低い頻度であった．

皮膚症状に関しては，白斑，顔面の血管線維腫，シャグリンパッチ，爪囲線維腫いずれも高頻度に認められ，中でも顔面の血管線維腫は89%で何れの年齢においても高頻度に認められた．

肺病変に関しては，100人中HRCTを施行した62人に関して検討した．全てHRCTによる診断であるが，MMPH（Multifocal Multinodular Pneumocyste Hyperplasia）か，LAM（Lymphangiomyomatosis）のいずれかを有する頻度は74%と従来考えられていたのとは桁違いに多かった．

腎病変に関しては，100人中エコーや腹部CT，MRIで検索した患者88人について検討した．その結果，血管筋脂肪腫が44%，嚢腫27%，腎癌3%，何れの腎病変も認められなかった患者は28%であり，腎病変も高頻度に認められた．

以上より，TSCでは，精神発達遅滞や痙攣発作の割合が減少し，逆に腎病変や肺病変の頻度が増加しており，従来小児科でみられていた患者と皮膚科の患者では，その構成に違いがあると思われた．さらに皮膚症状はいずれも高頻度に認められ，皮膚症状の本症診断における重要度の増加が示唆された．

TSCの診断

TSCは先天異常ではあるが，必ずしも全ての症状が生下時より出現するわけではなく，症状にばらつきが多く，特異性も低い．従って，本症の診断はいくつかの症状を組み合わせて行う．通常，本症の診断には1998年7月にMarylandのAnnapolisで開催されたTSCのConsensus Conferenceで批准された診断基準を用いる（表1）[5]．日本皮膚科学会における診断基準もこれを適用している．

TSCの症状，治療

心臓の横紋筋腫は胎生期に出現し出生時に最も著明になり，その後縮小していく．従って，心横紋筋腫は乳児期の重要な病変ではあるが，皮膚科医がその診断や治療を必要とされることは稀である．

皮膚症状は白斑，顔面の血管線維腫，シャグリンパッチ，爪囲線維腫等であり，白斑以外は思春期以降に著明になることが多いが，高頻度に出現し診断的に重要

大阪大学医学部皮膚科学教室
著者連絡先：（〒565-0871）大阪府吹田市山田丘2—15
大阪大学医学部皮膚科学教室　金田　眞理

表1　結節性硬化症の診断基準
（1998年の結節性硬化症のconsensus conferenceで批准）

大症状
1. 顔面の血管線維腫または前額部，頭部の結合織よりなる局面
2. 非外傷性多発性爪囲線維腫
3. 3つ以上の低色素斑
4. シャグリンパッチ（shagreen patch/connective tissue nevus）
5. 多発性の網膜の過誤腫（multiple retinal nodular hamartomas）
6. 大脳皮質結節（cortical tuber）*1
7. 脳室上衣下結節（subependymal nodule）
8. 脳室上衣下巨大細胞性星状細胞腫（subependymal giant cell astrocytoma）
9. 心の横紋筋腫（cardiac rhabdomyoma）
10. 肺リンパ管筋腫症（lymphangiomyomatosis）*2
11. 腎血管筋脂肪腫（renal angiomyolipoma）*2

小症状
1. 歯エナメル質の多発性小腔（multiple, randomly distributed dental enamel pits）
2. 過誤腫性直腸ポリープ（hamartomatous rectal polyp）*3
3. 骨シスト（bone cyst）*4
4. 放射状大脳白質神経細胞移動腺（cerebral white matter radial migration lines）*1,4,5
5. 歯肉の線維腫（gingival fibromas）
6. 腎以外の過誤腫（nonrenal hamartoma）*3
7. 網膜無色素斑（retinal achromic patch）
8. 散在性小白斑（confetti skin lesions）
9. 多発性腎嚢腫（multiple renal cyst）*3

*1 cortical tuberとcerebral white matter radial migration linesの両症状を同時に認める場合は1つと考える．
*2 lymphangiomyomatosisとrenal angiomyolipomaの両症状がある場合はDefinitive TSCと診断するには他の症状を認める必要がある．
*3 組織診断があることが好ましい．
*4 レントゲン所見で充分である．
Definitive TSC：大症状2つ，または大症状1つと小症状2つ
Probable TSC：大症状1つと小症状1つ
Possible TSC：大症状1つ，または小症状2つ以上

である．白斑は通常生下時から生後数カ月以内に出現するが不完全脱色素斑で，特に治療を用しない．

顔面の血管線維腫は5歳以上のTSC患者の80%以上に認められ，乳幼児期にはvascular spider様の病変として認められる事が多い．思春期頃より皮疹が増加増大する．美観を損なうものに対しては，液体窒素療法，レーザ治療，アブレージョン，外科的切除を施行．シャグリンパッチは疣様の小腫瘤の散在として認められることもある．背部，特に腰仙部の10センチメートル以上の大きなものは外科的切除の適応となる．

爪囲線維腫は通常思春期以降に出現し，徐々に増大する．日常生活の障害となる場合は外科的切除の対象となるが，切除してもすぐ再発してくる．

精神神経学的症状はTSCの重要な症状の一つであるが，痙攣発作や精神発達遅滞，自閉症などの行動異常は皮膚科受診前に診断治療をされており，むしろ皮膚科で問題になるのはそれらの症状のない患者のSubependimal Giant Cell Astrocytoma（SEGA）である．脳室周囲に多くSEGAは小児期から思春期にかけて急速に増大する事が多い為，自覚症状のない場合でもCTやMRI等の検査を行い，所見があった場合は大きさや部位によって，半年から1年に一回フォローをし，増大傾向があれば専門医を紹介する．

TSC患者の80%以上が何らかの腎病変を持っており，嚢腫，血管筋脂肪腫（Angiomyolipoma；AML）腎癌が本症に特徴的な病変である．腎嚢腫は両側多発性で，小児期に発症することが多い．臨床的には，腎機能障害および高血圧の原因となる．AMLも両側多発性で，臨床的には無症状で，特殊な場合を除いては血液検査では異常は認められず，腎機能障害が出現する

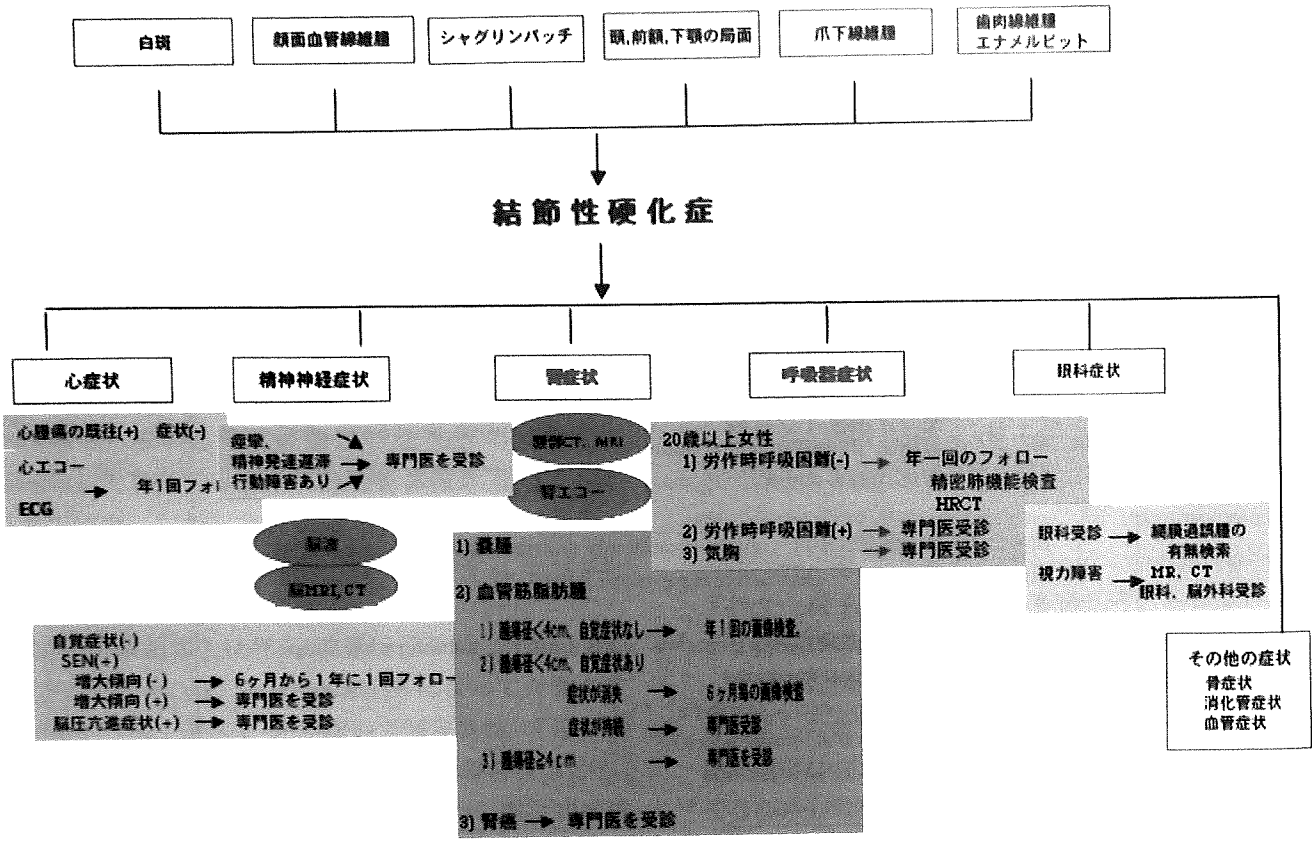

図1 結節性硬化症の診断手順

ことも少ない．腫瘍の発育は様々であるが，特に10代では急速に増大することが多く，突然後腹膜への大量出血を起こしてショック症状に陥ることもある．特に腫瘍径が4cm以上の場合は腫瘍サイズが増大しやすく，自然破裂の頻度も高くなる為，CTやエコーによる定期的な検査フォローが不可欠である．治療方針の選択に際しては，大きさと自覚症状により図のような対応が望ましい（図1）．

TSCの腎腫瘍は通常良性腫瘍であるが，腫瘍増大時にはその一部より悪性腫瘍の出現をみることがある．多くは血管筋脂肪腫と混在し両側多発性である．

肺症状に特徴的なのはmultifocal micronodular type 2 pneumocyte hyperplasia（MMPH））とpulmonary Lymphangiomyomatosis（LAM）である．MMPHは2型肺胞上皮細胞の過形成が肺内に瀰慢性におこってくる状態で，肺のHRCT検査でしばしば認められる．特に治療は要しないが，粟粒結核や一部の肺腫瘍等との鑑別が必要である．LAMは40歳以上の結節性硬化症患者の主な死因のひとつで，進行性で予後不良とされているが軽症例が増加している．時に繰り返す気胸で発症することもあるが，通常無症状で進行しないと単純胸部X線では異常が認められない．HRCTと精密肺機能検査で早期に変化が認められる．従って20歳以上のTSC患者特に女性患者では，自覚症状がなくても年1回はこれらの検査をスクリーニング的に施行し，肺HRCTで両側対称性のparenchymaの増強，cystic appearanceやhoneycomb像など嚢胞性変化の有無を，又，精密肺機能検査ではFEV1, FEV1/FVC, DL_{CO}の低下の有無をフォローし，異常を認めた場合や自覚症状がある場合には速やかに呼吸器内科専門医の受診を勧めるのが望ましい．

約50%の患者に網膜や視神経の過誤腫が認められ，まれに視力障害を生じることもある為，一度は眼科の専門医を受診するのが望ましい．頬粘膜，歯肉，舌底面，口蓋の腫瘍，歯のenamel defect（enamel pit）と呼ばれる小さなエナメル質の欠損，症状を伴わない骨の硬化像や，直腸の線維腫性ポリープ，肝腺腫，脾臓や子宮の過誤腫等を認めることがあるので必要に応じて精査をする．

現時点ではTSCに対する確実かつ有効な治療法はなく，世界的にはラパマイシン等のmTOR阻害剤の使用が試みられており[6][7]今後我が国においても使用

を考えていくべきと思われる.

文　献

1) Gunther M, Penrose LS: The genetics of epiloia, *J Genet*, **31**: 413–430, 1935.
2) The Europian chromosome 16 Tuberous Sclerosis Consortium: Identification and characterization of tuberous sclerosis gene on chromosome.
3) van Slegtenhorst M, et al: Identification of The Tuberous Sclerosis Gene *TSC1* on Chromosome 9q34, *Science*, **277**: 805–808, 1997.
4) 結節性硬化症の診断基準・治療ガイドライン作成委員会：結節性硬化症の診断基準および治療ガイドライン，日皮会誌，**118**：1667–1676, 2008.
5) Roach ES, et al: Tberous sclerosis complex consensus conference: revised clinical diagnostic criteria, *J Child Neurol*, **13**: 624–628, 1998.
6) Franzuberous sclero DTN, et al: Rapamycin Causes regression of Astrocytoma in Tuberous Sclerosis Complex, *Ann Neurol*, **59**: 490–495, 2006.
7) Bissler JJ, et al: Sirolimus for Angiomyolipoma in Tuberous Sclerosis complex or Lymphangioleiomyomatosis, *N Eng J Med*, **358**: 140–151, 2008.

After initial treatment with systemic prednisone, our patient's lesions and symptoms improved. Two months after diagnosis, his condition was stable under treatment with prednisone and mycophenolate mofetil. The present report of an adult man with concurrent SS and new-onset SLE reminds clinicians that this phenomenon, albeit rare, should always be considered, given suggestive clinical and laboratory signs and symptoms.

Neil F. Fernandes, MD
Leslie Castelo-Soccio, MD, PhD
Ellen J. Kim, MD
Victoria P. Werth, MD

Correspondence: Dr Werth, Department of Dermatology, University of Pennsylvania, Perleman Center for Advanced Medicine, 3400 Civic Center Blvd, Ste 1-330S, Philadelphia, PA 19104 (werth@mail.med.upenn.edu).
Financial Disclosure: None reported.
Funding/Support: This study was supported in part by National Institutes of Health grant NIH K24-AR 02207 (Dr Werth).

1 Hou TY, Chang DM, Gao HW, Chen CH, Chen HC, Lai JH Sweet's syndrome as an initial presentation in systemic lupus erythematosus a case report and review of the literature. *Lupus* 2005;14(5).399-402.
2 Burnham JM, Cron RQ. Sweet syndrome as an initial presentation in a child with systemic lupus erythematosus *Lupus*. 2005,14(12).974-975
3. Camarillo D, McCalmont TH, Frieden IJ, Gilliam AE Two pediatric cases of nonbullous histiocytoid neutrophilic dermatitis presenting as a cutaneous manifestation of lupus erythematosus *Arch Dermatol* 2008;144(11)·1495-1498
4. Callen JP. Neutrophilic dermatoses *Dermatol Clin* 2002,20(3):409-419.
5 Rahman A, Isenberg DA. Systemic lupus erythematosus *N Engl J Med*. 2008, 358(9) 929-939
6. Su WP, Liu HN. Diagnostic criteria for Sweet's syndrome Cutis. 1986,37(3)· 167-174.

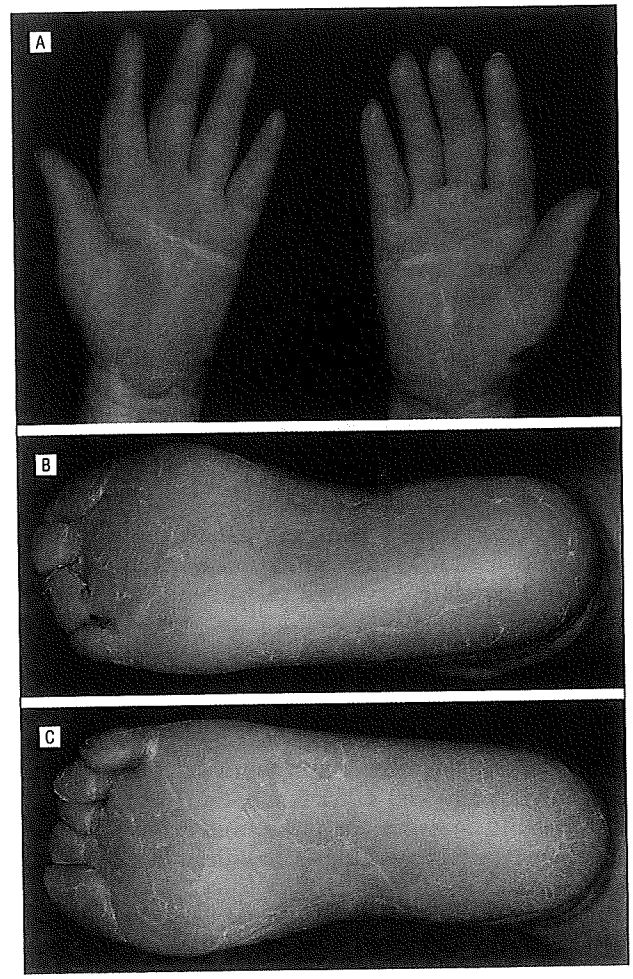

Figure 1. The palms (A) and soles (B and C) showed diffuse thick hyperkeratosis with erythematous border. The black spot on the thenar eminence of the palm is subcutaneous bleeding.

Epidermolytic Palmoplantar Keratoderma With Constriction Bands on Bilateral Fifth Toes

Epidermolytic palmoplantar keratoderma (EPPK) is an autosomal dominant skin disorder characterized by hyperkeratosis limited to the palms and soles and can be categorized into 2 types: Vörner and Unna-Thost types. The clinical expressions of the 2 types of EPPK are similar, but the histologic characteristics are different. Vörner type EPPK is characterized by vacuolar degeneration of keratinocytes in the upper spinous to granular layers. Unna-Thost EPPK can be distinguished from Vörner type because the Unna-Thost type lacks vacuolar degeneration.

Report of a Case. A 63-year-old woman was admitted to our hospital in April 2007 with thickened and yellowed palms and soles (**Figure 1**). She explained that her paternal grandfather, her father, and her daughter were similarly affected, but none of her family had received treatment for the condition. She reported that over the last 5 years, her fifth toes bilaterally showed slowly developing pseudoainhumlike constriction bands (**Figure 2**). Her teeth, oral mucosa, nails, and hair were all normal, as were the findings of her general physical examination. A skin biopsy specimen

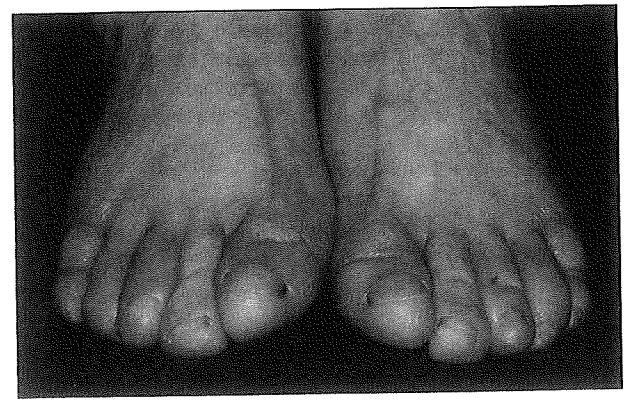

Figure 2. Pseudoainhumlike constriction bands on both fifth toes.

from her left sole showed remarkable hyperkeratosis and slight vacuolar degeneration of keratinocytes in the granular layers.

We isolated genomic DNA from the patient's peripheral blood by using standard techniques. Mutation identification was performed by direct sequencing of polymerase chain reaction (PCR) products. Genomic DNA was amplified using the following: 1 µL of GeneAmp dNTP (Applied Biosystems, Foster City,

California), 2.5 μL of GeneAmp10×PCR Buffer (Applied Biosystems), and 3.0 μL each of 25mM magnesium chloride and Taq polymerase (AmpliTaq Gold; Applied Biosystems). The forward keratin 9 primer sequence used was 5′-TTG GCT ACA GCT ACG GCG GAG GAT-3′; reverse, 5′-TGA GAT CAT CAA TAG TGT TAT AAT-3′.[1] The PCR program involved 1 cycle at a temperature of 94°C for 5.5 minutes; 1 cycle at 62°C for 1.0 minute; 1 cycle at 72°C for 1.0 minute; 1 cycle at 94°C for 0.5 minute; 1 cycle at 62°C for 1.0 minute; 40 cycles at 72°C for 1 minute each; and 1 cycle at 72°C for 10 minutes in a PTC-100 Programmable Thermal Controller (MJ Research Inc, Watertown, Massachusetts). Polymerase chain reaction products were purified using QIA Quick PCR purification Kit (Qiagen, Hilden, Germany).

The genomic DNA from the patient's peripheral blood showed an R162W mutation in the keratin 9 gene. We therefore diagnosed the patient with Vörner type EPPK.

Comment. Our case was diagnosed by clinical, histologic, and genetic findings as Vörner type EPPK; this diagnosis was made despite the clinical finding of pseudoainhumlike constriction bands on the both fifth toes. Interestingly, no other family members had this skin sign. As far as we are aware, this is the first case of Vörner type EPPK with pseudoainhumlike constriction bands.[2-5]

The expression of keratin 9 might vary individually at the boundary between the sole and the instep. Our patient had hyperkeratosis and an erythematous border not only of palms and soles but also on parts of the dorsal surfaces of the fingers and toes. It might be speculated that keratin 9 expression on the dorsal surfaces of the fingers and toes in this patient is related to the distribution of a subset of keratin 9–inducible dermal fibroblasts.[5] It might be also speculated, given her genetic background, that the pseudoainhumlike constriction bands were caused by her wearing high heels and tight sandals.

Naoko Funakushi, MD
Nobuyasu Mayuzumi, MD, PhD
Ryohei Sugimura, MD
Shigaku Ikeda, MD, PhD

Correspondence: Dr Funakushi, 2-1-1 Hongo, Bunkyo-ku, Tokyo, 113-8421, Japan (nao2794@juntendo.ac.jp).
Financial Disclosure: None reported.

1 Covello SP, Irvine AD, Mckenna KE, et al Mutation in keratin K9 in kindreds with epidermolytic palmoplantar keratoderma and epidemiology in Northern Ireland. *J Invest Dermatol* 1998;111(6).1207-1209.
2 Kon A, Itagaki K, Yoneda K, Takagaki K A novel mutation of keratin 9 gene (R162P)in a Japanese family with epidermolytic palmoplantar keratoderma *Arch Dermatol Res* 2005,296(8):375-378.
3 Terrinoni A, Cocuroccia B, Gubinelli E, et al. Identification of keratin K9 R162W mutation in patients of Italian origin with epidermolytic palmoplantar keratoderma *Eur J Dermatol* 2004;14(6) 375-378
4 Reis A, Hennies HC, Langbein L, et al. Keratin 9 gene mutation in epidermolytic palmoplantar keratoderma (EPPK). *Nat Genet.* 1994,6(2) 174-179.
5 Yamaguchi Y, Itami S, Tarutani M, Hosokawa K, Miura H, Yoshikawa K Regulation of keratin 9 nonpalmoplantar keratinocytes by palmoplantar fibroblasts through epithelial-mesenchymal interactions *J Invest Dermatol* 1999, 112(4).483-488

Efficacy of Adalimumab in the Treatment of Generalized Granuloma Annulare in Monozygotic Twins Carrying the 8.1 Ancestral Haplotype

Granuloma annulare (GA) is a condition of unknown cause characterized by the appearance of cutaneous necrobiotic granuloma. Localized forms of GA are usually asymptomatic and self-limited, with spontaneous resolution occurring often within 2 years. However, disseminated GA (DGA) tends to be more chronic and pruritic and may last for decades.

Some investigations have shown that an overexpression of tumor necrosis factor α (TNF-α) by peripheral mononuclear lymphocytes and macrophages may play a role in the development of GA.[1] Tumor necrosis factor α blocking agents such as etanercept and infliximab have helped resolve the disease in some cases.[2,3] In others, however, no response or a worsening of the condition was reported.[4] The reason for this varying response remains unknown.

Herein, I report a case of rapid improvement of DGA in identical twin sisters who were treated with the TNF-α blocking agent adalimumab. The twins were found to carry the human ancestral haplotype 8.1 (AH8.1), a genotype that has been associated with TNF-α polymorphisms leading to increased production of TNF-α by peripheral blood mononuclear cells.[5] A PubMed search revealed no previous use of adalimumab in the effective treatment of GA.

Report of a Case. A 67-year-old healthy white woman presented with a 2-year history of gradual-onset, generalized pruritic eruption. Her family history was significant for DGA in her identical twin.

Physical examination revealed hundreds of erythematous waxy papules, macules, and plaques on the extremities and torso, clinically consistent with DGA (**Figure 1**A). A biopsy specimen of 1 of the lesions revealed changes typical of GA (**Figure 2**).

Treatment with topical and oral corticosteroids, topical macrolides, dapsone, and hydroxychloroquine yielded no improvement in her condition or was associated with unacceptable adverse effects. On the basis of studies reporting successful treatment of idiopathic granulomatous diseases with TNF-α blocking agents,[3,4,6] we treated the patient with adalimumab, 40 mg/wk, for 3 months to determine efficacy. This therapy yielded rapid improvement: all of the truncal lesions resolved within 2 months and most of the remaining older macular lesions on the distal extremities faded within 3 months (Figure 1B). Six months later, the patient remained free of recurrence. Her sister was offered a trial of adalimumab as well, and a similar response was achieved.

To determine if our patient and her sister possessed human leukocyte antigen (HLA) markers previously reported in patients with generalized GA, we tested them both for antigens in the HLA-A, HLA-B, and

Human Pathology (2009) 40, 430–434

ELSEVIER

Human PATHOLOGY

www.elsevier.com/locate/humpath

Case study

Dissociate expression of tuberous sclerosis complex 1 product hamartin in a skin and pulmonary lesion of a tuberous sclerosis complex☆

Mari Wataya-Kaneda MD, PhD*, Ichiro Katayama MD, PhD

Department of Dermatology, Osaka University Graduate School of Medicine, Suita-shi, Osaka 565-0871, Japan

Received 30 January 2008; revised 7 May 2008; accepted 23 June 2008

Keywords:
Tuberous sclerosis complex;
Hamartin;
Loss of heterozygosity, (LOH);
Lymphangiomyomatosis, (LAM);
Tuberin

Summary Tuberous sclerosis complex is a multisystemic disorder characterized by systemic hamartomas. Tuberous sclerosis complex is caused by the mutation of tumor suppressor genes tuberous sclerosis complex 1 or tuberous sclerosis complex 2. Tuberous sclerosis complex tumorigenesis is not always accompanied by loss of heterozygosity. The incidence of loss of heterozygosity is varied among the organs in which hamartomas occur. We report a 25-year-old woman diagnosed with tuberous sclerosis complex with lymphangiomyomatosis. Expression of tuberin and hamartin was examined in lung and skin specimens. Her skin lesion (angiofibroma) expressed both hamartin and tuberin, but her pulmonary lesion did not express hamartin. This suggests that different mechanisms of tumorigenesis may occur in pulmonary and skin lesions.

1. Introduction

Tuberous sclerosis complex (TSC) is a multisystemic disorder characterized by systemic hamartomas and involves many organs, including lung and skin. Pulmonary involvement in TSC includes lymphangiomyomatosis (LAM) and multifocal micronodular pneumocyte hyperplasia [1-3]. LAM is a progressive lung disease characterized by a diffuse proliferation of abnormal alveolar smooth muscle cells and cystic destruction of parenchyma. LAM predominantly affects females of childbearing age. The most common symptoms are dyspnea and pneumothorax. No symptoms are seen in early stages of LAM. High-resolution computed tomography (HRCT) and pulmonary function tests are the most sensitive tools for recognizing LAM before the development of symptoms [1,4]. TSC-LAM is associated with a *TSC* germline mutation [5], and loss of heterozygosity (LOH) on this allele causes the disease. Skin lesions include facial angiofibroma, hypomelanotic macules, shagreen patches, and ungual fibromas. LOH in facial angiofibromas appears to be uncommon [6].

Herein, we report a patient with TSC with LAM. Her pulmonary lesion did not express hamartin, the *TSC1* product, but her skin lesion expressed both hamartin and tuberin. We performed mutation analysis of the patient in the *TSC1* and *TSC2* genes using single-strand conformational polymorphism analysis and direct sequencing according to the method described previously [7]. No mutation was found

☆ This work was supported by grant from Japanese Ministry of education, culture, sports, science and technology for M. Wataya-Kaneda, and grant from Japanese Ministry of health, labors and welfare for I. Katayama.

* Corresponding author
E-mail address: mkaneda@derma.med.osaka-u.ac.jp (M. Wataya-Kaneda).

0046-8177/$ – see front matter © 2009 Elsevier Inc. All rights reserved.
doi:10.1016/j.humpath.2008.06.026

in either gene. This demonstrated that different mechanisms of tumorigenesis might occur in skin and pulmonary lesions.

2. Case report

A 25-year-old Japanese woman complained of chest pain. A chest roentgenogram revealed bilateral pneumothorax. Although she had an approximately 20-year history of TSC, she had no respiratory symptoms. She also had no epilepsy or mental retardation. She had facial angiofibromas, shagreen patches, hypomelanotic macules, ungual fibromas, and gingival fibromas (Fig. 1A and Table 1). Brain magnetic resonance imaging showed cortical tubers. Computed tomography (CT) demonstrated calcified subependymal nodules (Fig. 1B). Abdominal CT revealed a bilateral multiple hypodense mass, which was suspected to be renal angiomyolipomas (Fig. 1C). Her pulmonary function test showed a slight obstructive pattern, and HRCT of her chest showed multiple thin-walled cysts distributed diffusely throughout both lungs (Fig. 2A). Because the patient had a clinical history of TSC, an open lung biopsy was performed during the surgical treatment of pneumothorax for the investigation of LAM. Specimens from pulmonary lesions were formalin fixed, paraffin embedded, cut at 4 μm, put on slide glasses, and dried. After being deparaffinized and hydrated, the specimens were stained immunohistochemically using anti-HMB-45 antibody (Dako,

Table 1 Clinical diagnostic criteria

Major features
1. Facial angiofibroma
2. Nontraumatic ungual or periungual fibroma
3. Hypomelanotic macules (>3)
4. Shagreen patch/connective tissue nevus
5. Multiple retinal nodular hamartomas
6. Cortical tuber
7. Subependymal nodule
8. Subependymal giant cell astrocytoma
Minor features
1. Multiple randomly distributed dental enamel pits
2. Hamartomatous rectal polyp
3. Bone cyst
4. Cerebral white matter radial migration lines
5. Gingival fibromas
6. Nonrenal hamartoma
7. Retinal achromic patch
Definitive TSC: either 2 major features or one major feature plus 2
Probable TSC: one major plus one minor feature
Possible TSC: either one major feature or 2 or more minor features
Criteria for germline mosaicism
1. Couples with more than one child with tuberous sclerosis complex
2. No extended family history
Clinical symptoms shown on the patient were underlined

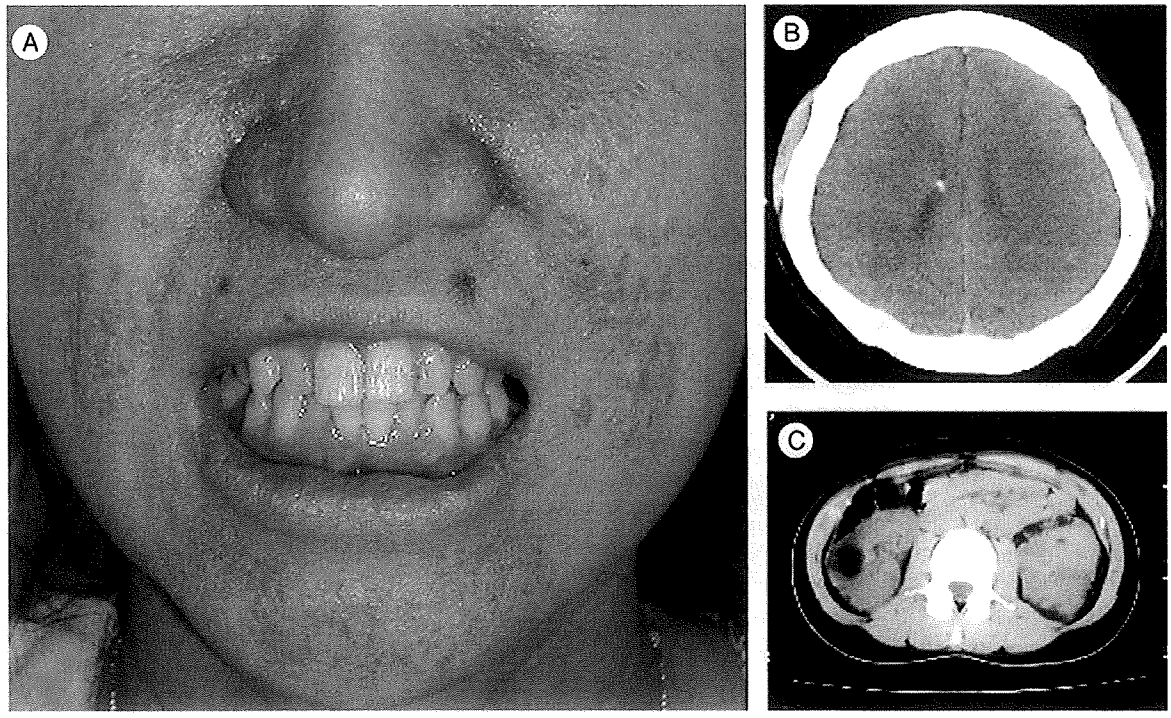

Fig. 1 Diagnostic appearance of clinical and radiologic features. A, Facial angiofibromas and gingival fibromas. B, The brain CT image demonstrated calcification along the ventricle. C, The abdominal CT showed a bilateral multiple hypodense mass in the kidney

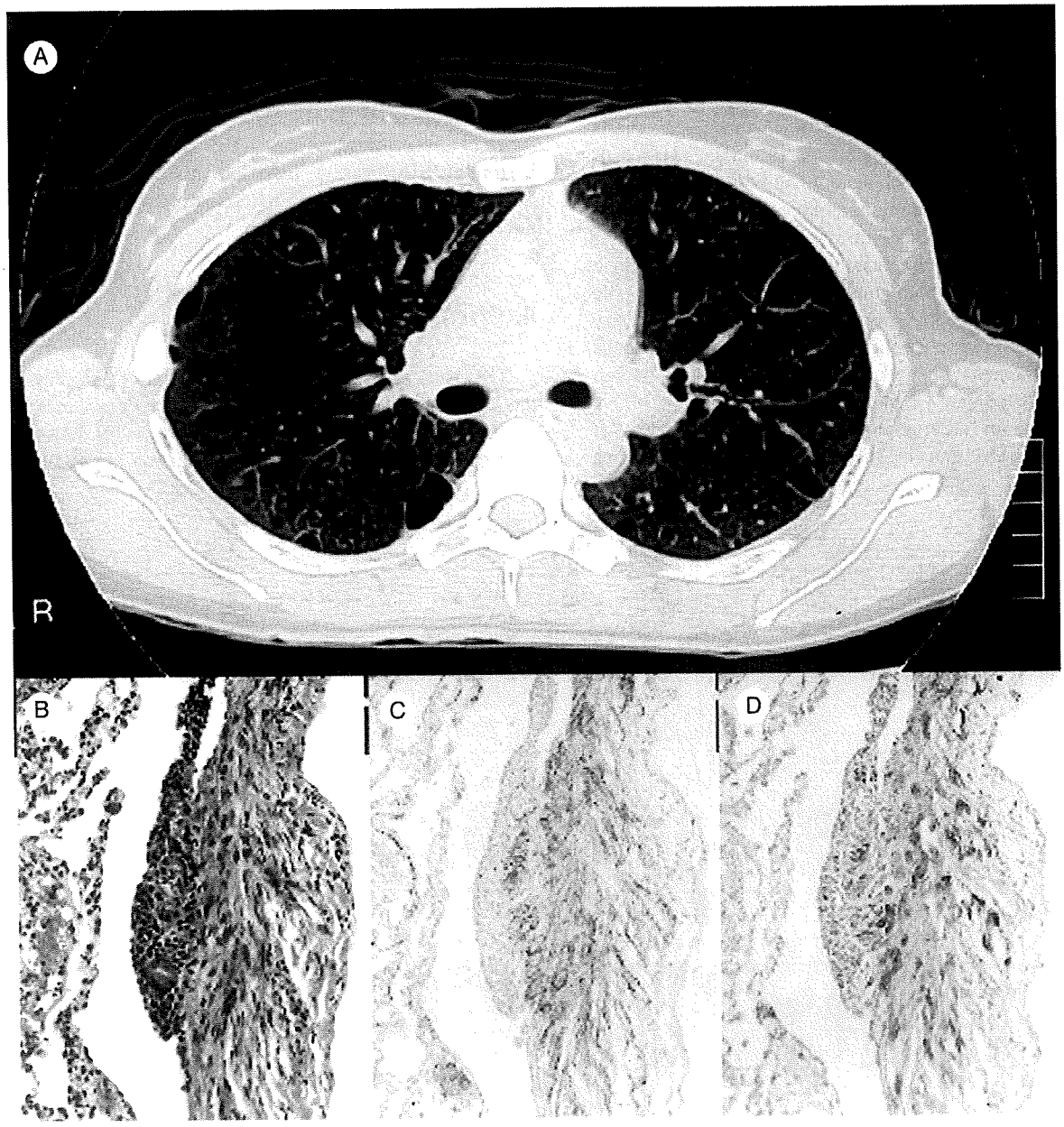

Fig. 2 Radiologic and pathologic features of pulmonary LAM. A, A chest HRCT scan showed multiple thin-walled cysts surrounded by normal parenchyma scattered throughout both lungs. B, Immunohistochemistry of LAM cells H&E stain. C, Immunohistochemical staining with anti-α-SMA antibody. D, Immunohistochemical staining with anti-HMB-45 antibody. Small foci of spindle-shaped cells that were stained by both anti-α-SMA and anti-HMB-45 antibodies were identified on the thickened septa of some abnormal cysts.

Glostrup, Denmark) and anti-human α-smooth muscle actin (α-SMA) antibody (Dako) with hematoxylin and eosin (H&E) staining. Primary antibodies were detected using Dako REALEnVision Detection System, Peroxidase/DAB+, Rabbit/Mouse (Dako). Counterstaining was done using methyl green (Dako). To define the LAM, we performed a microscopic examination. The H&E staining specimen showed cystic destruction of the parenchyma and thickening of alveolar septa, which were composed of spindle-shaped cells (Fig. 2B). Immunohistochemical examination revealed that the abnormal spindle-shaped cells expressed both HMB-45 and α-SMA and were, therefore, identified as LAM cells (Fig. 2C, D). To show the expression of hamartin and tuberin on the skin and pulmonary lesions, we stained specimen from skin lesions that has been obtained 1 year before the lung biopsy and pulmonary lesions using antihamartin (Santa Cruz Biotechnology, Santa Cruz, CA) and antituberin antibodies (Santa Cruz Biotechnology). Primary antibodies were detected as described above, and counterstaining was done with hematoxylin.

3. Results

Herein, we reported a patient with TSC with LAM. The diagnosis of TSC was based on the clinical diagnostic criteria agreed by the Tuberous Sclerosis Complex Consensus Conference in 1998 [8]. The patient had 8 major symptoms, including LAM, and one minor symptom (Table 1) and was therefore diagnosed with definitive TSC. The diagnosis of LAM was based on the histopathologic features, which showed abnormal smooth muscle proliferation and cystic destruction in the H&E specimen. Immunohistochemistry indicated the presence of abnormal smooth muscle–like cells positively stained with both HMB-45 and α-SMA, which indicates that they are LAM cells (Fig. 2B-D).

Expression of tuberin and hamartin in the lesions of pulmonary LAM and in the facial angiofibromas was examined using antituberin and antihamartin antibodies. Only tuberin was expressed in LAM cells (Fig. 3A-C), but both tuberin and hamartin were expressed in the facial angiofibroma (Fig. 3D-I).

To examine the genotype of TSC, mutation analysis was performed. However, no mutation was found on *either the TSC1 or the TSC2* gene. LOH on the pulmonary lesion was not confirmed.

4. Discussion

TSC is an autosomal dominant disorder characterized by the development of hamartomas in many organs, including the brain, eyes, kidneys, heart, lungs, and skin [9]. It has been reported that TSC is caused by the mutation in one of the 2

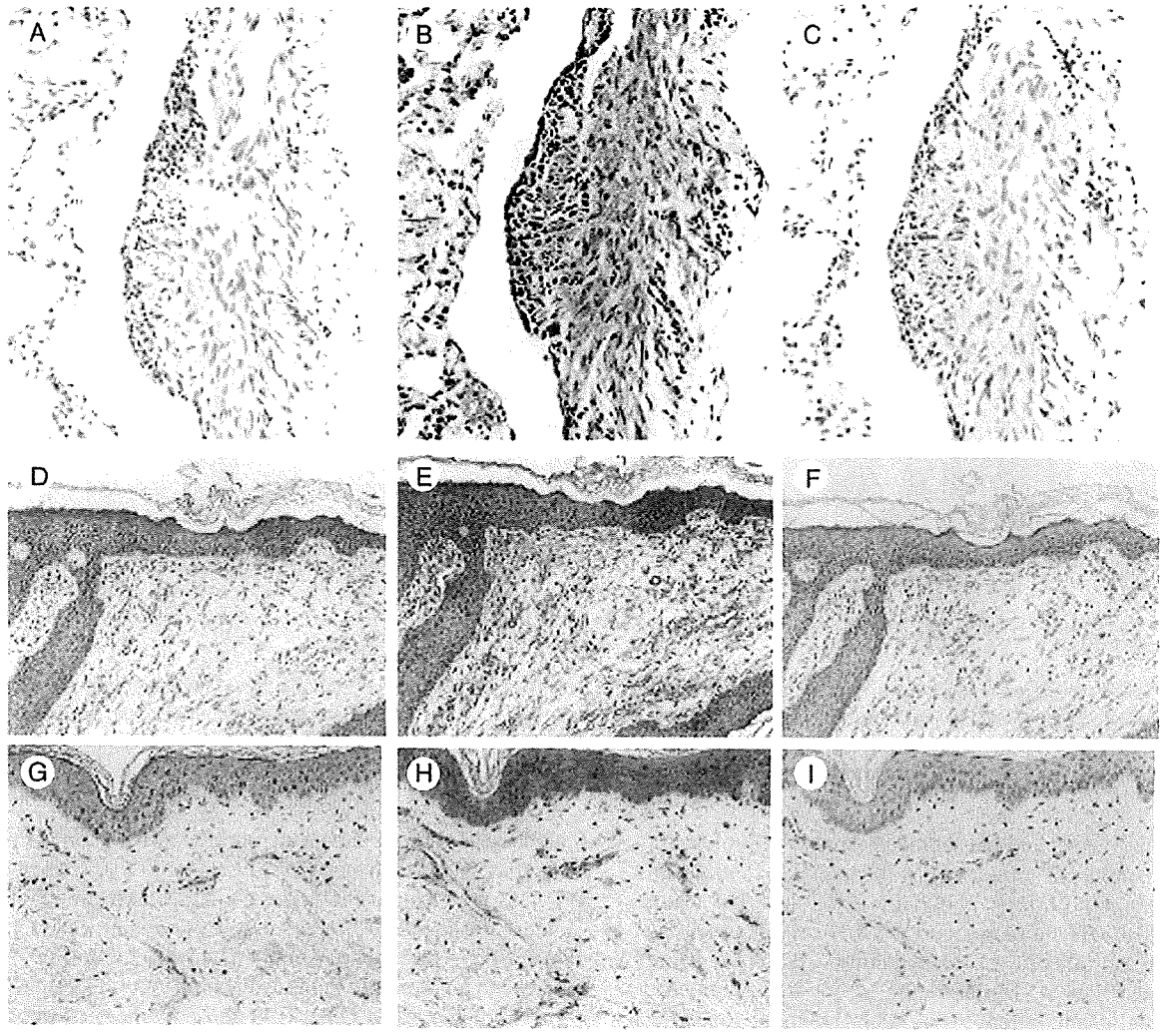

Fig. 3 Expression of hamartin and tuberin in LAM cells and on skin lesions. LAM cells stained using (A) antihamartin and (B) antituberin antibodies. Facial angiofibroma stained using (D) antihamartin and (E) antituberin antibodies. Unaffected control skin stained using (G) antihamartin and (H) antituberin antibodies. C, F, I, Negative control.

tumor suppression genes *TSC1* or *TSC2*, encoding hamartin and tuberin. Mutation in either *TSC1* or *TSC2* gene equally contributes to this disorder [10]. Like other tumor suppressors, TSC hamartoma can be explained on the basis of Knudson's 2-hit theory [9,11]. In this theory, a second hit mutation resulting in LOH of the tumor suppressor gene is necessary for tumor formation. In fact, LOH is commonly found in several types of TSC hamartomas. TSC tumorigenesis is not always accompanied by LOH, and the incidence of LOH is different in each organ. LOH at either *TSC* gene locus is frequently detected in pulmonary LAM as well as in cardiac rhabdomyomas and renal angiomyolipomas [9]. In contrast, in brain lesions and skin lesions, the incidence of LOH is low [9,12,13]. Recently, many studies have reported evidence that somatic mutations resulting in the loss of wild-type alleles may not be necessary. Several hypotheses explained why, in spite of the presence of hamartin and tuberin, brain lesions formed hamartomas in TSC [14]. One hypothesis is the different localization of hamartin and tuberin in cells [15]. Separate cellular localization of hamartin and tuberin may prevent the formation of the hamartin-tuberin complex, resulting in mTOR activation. Another explanation is mosaicism. Some chromosomal changes exist only in a mosaic form, because in a nonmosaic form, they are lethal [10]. The third possibility is an epigenetic mechanism as reported previously [16]. Finally, extracellular signal-regulated kinase is also related to the TSC tumorigenesis in the lack of *TSC2* LOH [17].

In this case, the pulmonary lesion did not express hamartin, but the skin lesion expressed both hamartin and tuberin. Dissociation of hamartin expression in lung and skin lesions shows that different mechanisms of tumorigenesis may occur in different organs.

References

[1] Hancock E, Osborne J Lymphangioleiomyomatosis. a review of the literature Respir Med 2002;96·1-6

[2] Maruyama H, Seyama K, Sobajima J, et al Multifocal micronodular pneumocyte hyperplasia and lymphangioleiomyomatosis in tuberous sclerosis with a TSC2 gene. Mod Pathol 2001.14·609-14

[3] Maruyama H, Ohbayashi C, Hino O, et al Pathogenesis of multifocal micronodular pneumocyte hyperplasia and lymphangioleiomyomatosis in tuberous sclerosis and association with tuberous sclerosis genes TSC1 and TSC2. Pathol Int 2001;51 585-94.

[4] Hancock E, Tomkins S, Sampson J, et al Lymphangioleiomyomatosis and tuberous sclerosis. Respir Med 2002;96·7-13

[5] Strizheva GD, Carsillo T, Kruger WD, et al The spectrum of mutations in TSC1 and TSC2 in women with tuberous sclerosis and lymphangiomyomatosis. Am J Respir Crit Care Med 2001,163.253-8.

[6] Wataya-Kaneda M, Kaneda Y, Hino O, et al Cells derived from tuberous sclerosis show a prolonged S phase of the cell cycle and increased apoptosis. Arch Dermatol Res 2001.293 460-9

[7] Yamashita Y, Ono J, Okada S, et al Analysis of all exons of TSC1 and TSC2 genes for germline mutations in Japanese patients with tuberous sclerosis: report of 10 mutations Am J Med Genet 2000;90·123-6

[8] Roach ES, Gomez MR, Northrup H. Tuberous Sclerosis Complex Consensus Conference: revised clinical diagnostic criteria J Child Neurol 1998;13:624-8

[9] Green AJ, Smith M, Yates JR Loss of heterozygosity on chromosome 16p13 3 in hamartomas from tuberous sclerosis patients. Nat Genet 1994,6:193-6.

[10] Cheadle JP, Reeve MP, Sampson JR, et al. Molecular genetic advances in tuberous sclerosis. Hum Genet 2000.107·97-114.

[11] van Slegtenhorst M, de Hoogt R, Hermans C, et al Identification of the tuberous sclerosis gene TSC1 on chromosome 9q34 Science 1997;277:805-8

[12] Henske EP, Scheithauer BW, Short MP, et al Allelic loss is frequent in tuberous sclerosis kidney lesions but rare in brain lesions Am J Hum Genet 1996;59·400-6.

[13] Niida Y, Stemmer-Rachamimov AO, Logrip M, et al Survey of somatic mutations in tuberous sclerosis complex (TSC) hamartomas suggests different genetic mechanisms for pathogenesis of TSC lesions. Am J Hum Genet 2001;69 493-503.

[14] Jozwiak J, Jozwiak S. Giant cells contradiction to two-hit model of tuber formation? Cell Mol Neurobiol 2007;27.251-61.

[15] Jansen FE, Notenboom RG, Nellist M, et al. Differential localization of hamartin and tuberin and increased S6 phosphorylation in a tuber Neurology 2004,63:1293-5

[16] Han S, Santos TM, Puga A, et al Phosphorylation of tuberin as a novel mechanism for somatic inactivation of the tuberous sclerosis complex proteins in brain lesions. Cancer Res 2004,64·812-6

[17] Ma L, Chen Z, Erdjument-Bromage H, et al Phosphorylation and functional inactivation of TSC2 by Erk implications for tuberous sclerosis and cancer pathogenesis. Cell 2005;121 179-93

Molecular Vision 2009; 15:974-979 <http://www.molvis.org/molvis/v15/a102>
Received 5 August 2008 | Accepted 10 May 2009 | Published 15 May 2009

Double mutation (R124H, N544S) of *TGFBI* in two sisters with combined expression of Avellino and lattice corneal dystrophies

Naoyuki Yamada,[1] Koji Kawamoto,[1] Naoyuki Morishige,[1] Tai-ichiro Chikama,[2] Teruo Nishida,[1] Mitsuaki Nishioka,[3] Naoko Okayama,[3] Yuji Hinoda[3]

[1]Department of Ophthalmology, Yamaguchi University Graduate School of Medicine, Ube City, Yamaguchi, Japan, [2]Department of Ocular Pathophysiology, Yamaguchi University School of Medicine, Ube City, Yamaguchi, Japan; [3]Division of Laboratory, Yamaguchi University Hospital, Ube City, Yamaguchi, Japan

Purpose: The R124H mutation of the keratoepithelin gene (*TGFBI*) causes Avellino corneal dystrophy whereas the N544S mutation of this same gene gives rise to lattice corneal dystrophy. We now report two cases with both R124H and N544S mutations of *TGFBI*.

Methods: Genomic DNA and cDNA were isolated from the proband and family members and were subjected to polymerase chain reaction–mediated amplification of exons 1–17 of *TGFBI*. The amplification products were directly sequenced. Allele-specific cloning and sequencing were applied to evaluate the compound heterozygous mutation.

Results: Molecular genetic analysis revealed that the proband and one sister harbored both a heterozygous CGC→CAC (Arg→His) mutation at codon 124 and a heterozygous AAT→AGT (Asn→Ser) mutation at codon 544 of *TGFBI*. Slit-lamp examination revealed multiple granular regions of opacity and lattice lines in the corneal stroma of the proband and her sister with the double mutation. Allele-specific cloning and sequencing revealed that the R124H and N544S mutations are on different chromosomes.

Conclusions: As far as we are aware, this is the first report of a patient with a double mutation (R124H, N544S) of *TGFBI* causing an autosomal dominant form of corneal dystrophy. The clinical manifestations of the two cases with both R124H and N544S mutations appeared to be a summation of Avellino and lattice corneal dystrophies.

Mutations of the keratoepithelin gene (*TGFBI*) are responsible for most corneal dystrophies. *TGFBI* was first identified as a transforming growth factor-β1 (TGF-β1)-inducible gene in a human lung adenocarcinoma cell line [1]. The point mutations R124C, R124H, R555W, and R555Q of *TGFBI* were initially found to give rise to lattice corneal dystrophy (LCD), Avellino corneal dystrophy (ACD), Groenouw type I corneal dystrophy, and Reis-Bücklers corneal dystrophy, respectively [2]. Many additional mutations of *TGFBI* were subsequently found to be responsible for autosomal dominant corneal dystrophies [3, 4]. ACD is characterized by the presence of granular and linear opacities in the corneal stroma. The deposits in the corneal stroma of patients with ACD are of a hyaline and amyloid nature. The only identified mutation associated with ACD is R124H of *TGFBI* [2]. LCD is an inherited form of amyloidosis that is characterized by the development of lattice lines and opacities in the cornea. Several distinct mutations of *TGFBI* including R124C [2], L518P [5], P501T [6], L527R [7], N544S [8], A546T [9], and N622K (T1913G or T1913A) [3] have been associated with LCD. LCD is classified clinically into several subtypes [3,4], but standardized definitions of each subtype have not been achieved to date. The subtype of LCD caused by the N544S mutation of *TGFBI* is characterized by tiny nodular deposits with thin lattice lines in the middle portion of the corneal stroma [10].

Several case reports have suggested that corneal dystrophies caused by homozygous point mutations of *TGFBI* are characterized by an earlier onset, more severe symptoms, and a higher frequency of recurrence after keratoplasty compared with those attributable to the corresponding heterozygous mutations [11-15]. A few case reports have also described individuals with corneal dystrophy who harbor two distinct mutations in *TGFBI*, the membrane component, chromosome 1, surface maker 1 (*MISI*), or both [16-21]. It has remained unclear, however, how the phenotype of patients with such a double mutation differs from that of those with the corresponding single mutations. We now describe the first cases of corneal dystrophy associated with both R124H and N544S mutations of *TGFBI*.

METHODS

This study was approved by the ethical review committee for gene analysis research of Yamaguchi University School of Medicine and Yamaguchi University Hospital. After obtaining informed written consent, we extracted genomic DNA from white blood cells of peripheral blood collected from patients in the presence of an anticoagulant. Total RNA

Correspondence to Naoyuki Yamada, MD, PhD, Department of Ophthalmology, Yamaguchi University Graduate School of Medicine, 1-1-1 Minami Kogushi, Ube City, Yamaguchi, 755-8505, Japan, Phone +81-836-22-2278, FAX: +81-836-22-2334, email: n.yamada@po.cc.yamaguchi-u.ac.jp

TABLE 1. PCR PRIMERS USED FOR SEQUENCING EXONS OF *TGFBI*.

Exon	Primer	Primer sequence	Annealing temperature (°C)	Product size (bp)
2–9	cDNA-F1	5'-CGCCAAGTCGCCCTACCAG-3'	60	1205
	cDNA-R1	5'-TTGGAGGGGTTCCATCTTTG-3'		
9–17	cDNA-F2	5'-CTCATCCCAGACTCAGCCAA-3'	60	1075
	cDNA-R2	5'-CACATCTCATTATGGTGCGGC-3'		
1	DNA-1F	5'-CCGCTCGCAGCTTACTTAAC-3'	60	362
	DNA-1R	5'-AGCGCTCCAATGCTGCAAGGT-3'		
4	DNA-4F	5'-CGTCCTCTCCACCTGTAGAT-3'	62	350
	DNA-4R	5'-GACTCCCATTCATCATGCCC-3'		
11	DNA-11F	5'-CAGCCTTAATAACCCATCCCA-3'	58	375
	DNA-11R	5'-AATCCCCAAGGTAGAAGAAAG-3'		
12	DNA-12F	5'-AGGAAAATACCTCTCAGCGTGG-3'	60	293
	DNA-12R	5'-ATGTGCCAACTGTTTGCTGC-3'		
13	DNA-13F	5'-GGGAGTTCTTCATTTCAGGG-3'	58	365
	DNA-13R	5'-ATTACACTCAGAGATTCGGG-3'		
14	DNA-14F	5'-GCCTGGGCGACAAGATTGA-3'	58	419
	DNA-14R	5'-CCAACAGCTCCCAATTCAC-3'		

was also extracted from the white blood cells with the use of a QIAmp RNA Blood mini kit (Qiagen, Valencia, CA) and was then subjected to reverse transcription with the use of TaqMan Reverse Transcription Reagents (Applied Biosystems, Foster City, CA). The resulting cDNA as well as genomic DNA were subjected to polymerase chain reaction (PCR) with primers that amplify exons 1, 4, 11, 12, 13, 14, 2–9, or 9–17 of *TGFBI* (Table 1). Each PCR reaction was performed in a total volume of 10 µl containing template DNA (80 ng/µl), 10 pmol of each primer, 200 µM of each deoxynucleoside triphosphate, 20 mM $MgCl_2$, 20 mM Tris-HCl (pH 8.0), 100 mM KCl, and 1 U of Taq polymerase (Ex Taq; Takara, Tokyo, Japan). The reaction mixture was overlaid with 10 µl of mineral oil, and amplification was performed with a Gene Amp PCR System PC808 (ASTEC, Tokyo, Japan) with an initial denaturation at 95 °C for 2 min followed by 30 cycles of denaturation at 94 °C for 30 s, annealing at 58 °C, 60 °C, or 62 °C (Table 1) for 20 s, and extension at 72 °C for 30 s. The PCR products were separated by electrophoresis on a 2% agarose gel and stained with ethidium bromide. For sequencing, 2.5 µl of the PCR products were incubated with 1 µl of ExoSAP-IT (Amersham Bioscience, Tokyo, Japan) first for 20 min at 37 °C and then for another 20 min at 80 °C. Sequencing reactions were then performed with the use of a BigDye Terminator Cycle Sequencing FS Ready Reaction Kit (Applied Biosystems). After purification with ethanol, the reaction products were applied to an ABI 3100-Avant Genetic Analyzer (Applied Biosystems).

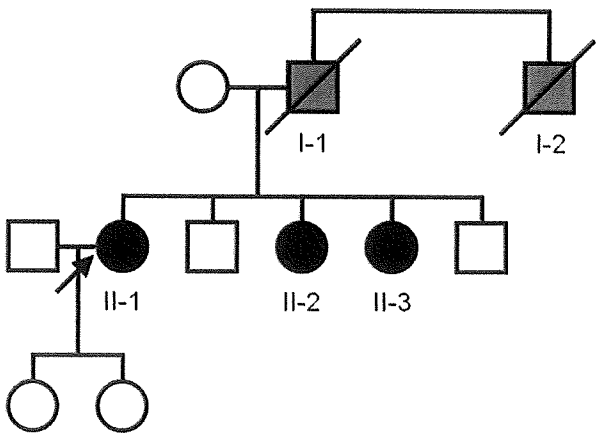

Figure 1. Pedigree of the proband Black symbols indicate individuals with a diagnosis of corneal dystrophy by genetic analysis Gray symbols indicate individuals suspected of having been affected by corneal dystrophy but not subjected to genetic analysis The arrow indicates the proband.

An allele-specific cloning and sequencing approach was applied to characterize the compound heterozygous mutation of R124H and N544S. In brief, cDNA of the proband was subjected to PCR with KOD FX DNA polymerase (Toyobo, Tokyo, Japan) and with the primers, 5'-TGT CCA GCA GCC CTA CCA CTC-3' (forward) and 5'-AGG ATA TCC CCT CTT TCC TGA GGT C-3' (reverse; containing an EcoRV restriction site at its 5' end), to obtain products that included both mutation sites. The PCR products were purified by electrophoresis and digested with EcoRV and BamHI (site in exon 4), and the released fragments were ligated into the multiple cloning site of a sequencing vector (pcDNA3.1[+]; Promega, Madison, WI). The resulting plasmids were expanded in competent *Escherichia coli* JM109 cells (Invitrogen, Carlsbad, CA), and the inserts were then sequenced as described above.

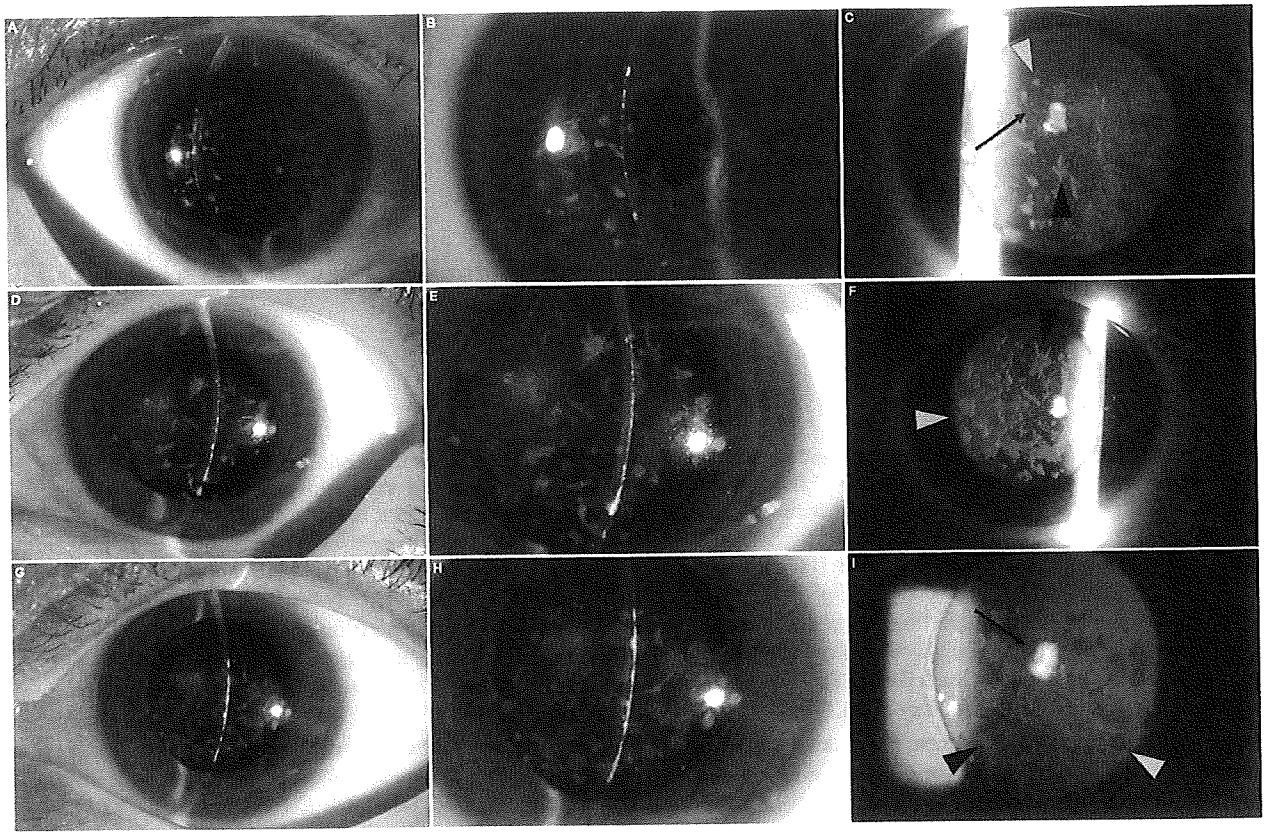

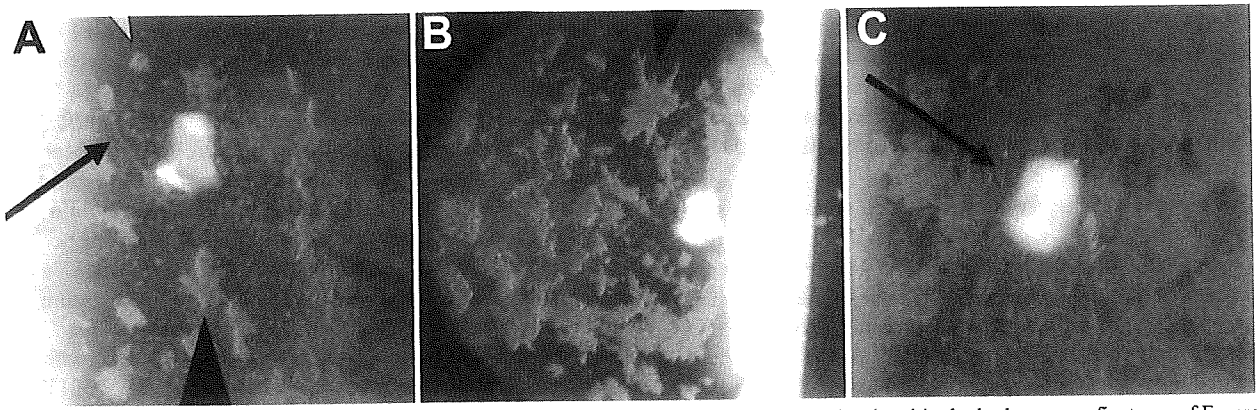

Figure 3 Lattice lines in patient's cornea The lattice lines referred to in Figure 2 are better visualized in the higher magnifications of Figure 2C, Figure 2F, and Figure 2I (Figure 3A-C, respectively) The lattice lines are easily seen in **A** and **C** (black arrows), but not in **B**

RESULTS

The proband, a 67-year-old Japanese woman (II-1), visited our corneal clinic in January 2000 with a main complaint of gradual impairment of vision (Figure 1). We diagnosed her condition as ACD on the basis of slit-lamp examination. Given that her visual acuity had decreased to 0.7 in the right eye and 0.4 in the left eye, we performed phototherapeutic keratectomy on her left eye in March 2000 and on her right eye in May 2000. The parents of II-1 were not related to each other. Her father (I-1) is no longer alive, and she has two

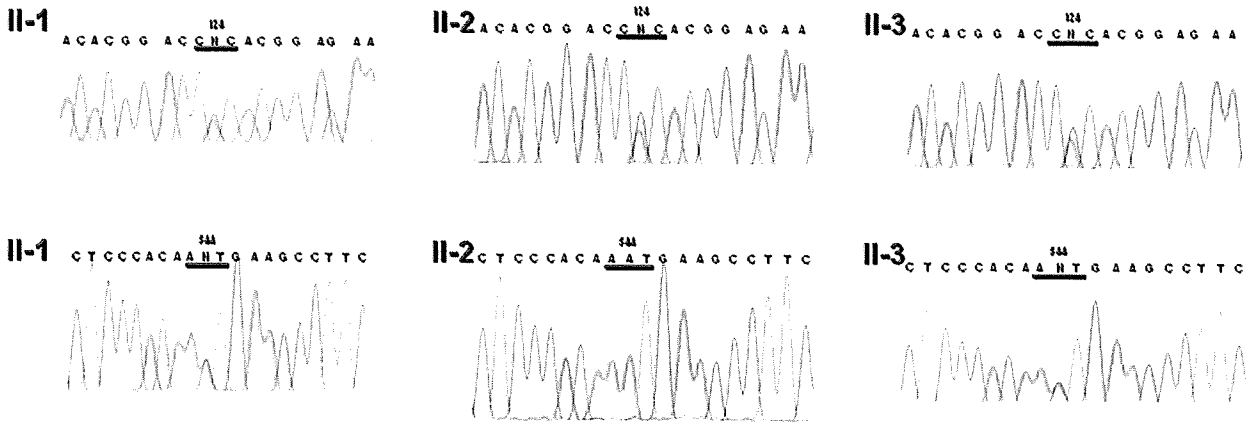

Figure 4 Genetic analysis of *TGFBI* in the proband and her two sisters Direct sequencing of genomic amplification products corresponding to exon 4 (upper panels) or exon 12 (lower panels) of *TGFBI* was performed for II-1, II-2, and II-3 A heterozygous CGC→CAC mutation was detected at codon 124 in II-1, II-2, and II-3 A heterozygous AAT→AGT mutation was detected at codon 544 in II-1 and II-3

brothers and two sisters. Her father's brother (I-2) and her sisters (II-2, II-3) were also diagnosed at our clinic with ACD by slit-lamp examination. Her reporting suggested that her father (I-1) had corneal dystrophy. We also performed phototherapeutic keratectomy on the left eye of II-2 in March 2000 and on the right eye of II-2 in May 2000.

Slit-lamp examination subsequently revealed multiple granular regions of opacity in the surface-to-middle portion of the corneal stroma in both eyes of II-1, II-2, and II-3. Lattice lines were also observed in II-1 (Figure 2A–C) and II-3 (Figure 2G–I) but not in II-2 (Figure 2D–F). These lattice lines can be seen better in the higher magnifications of Figure 2C, Figure 2F and Figure 2I (Figure 3A-C, respectively). Both II-1 and II-3 were found to harbor both a heterozygous CGC→CAC (Arg→His) mutation at codon 124 and a heterozygous AAT→AGT (Asn→Ser) mutation at codon 544 of *TGFBI* whereas II-2 harbored only the heterozygous CGC→CAC (Arg→His) mutation at codon 124 (Figure 4). The mutations were identified at both the genomic and cDNA levels.

To investigate whether the two *TGFBI* mutations are on the same or different chromosomes of the proband, we adopted an allele-specific cloning and sequencing approach. PCR products containing both mutation sites were subcloned and sequenced. Of three independent clones analyzed, one contained only the R124H mutation and the other two contained only the N544S mutation, indicating that the two mutations are on different chromosomes.

DISCUSSION

As far as we are aware, this is the first report of a patient with a double mutation of *TGFBI* causing an autosomal dominant form of corneal dystrophy. The clinical manifestations of the two cases with both R124H and N544S mutations appeared to be a summation of those of Avellino and lattice corneal dystrophies. We observed lattice lines in the corneas of II-1 and II-3, both of whom have the N544S mutation of *TGFBI*, but not in II-2, who harbors only the R124H mutation.

We were not able to perform genetic analysis on I-1 and I-2 because they were no longer alive at the time of this analysis. However, allele-specific cloning and sequencing revealed that the R124H and N544S mutations are on different chromosomes, consistent with our clinical findings. Slit-lamp examination of I-2 did not reveal the presence of lattice lines, suggesting that the R124H mutation was transmitted to the proband and her two sisters from I-1. Although slit-lamp examination was not performed on the mother of the three sisters because of her being confined to bed, it is likely that she harbors the N544S mutation of *TGFBI*. Given that the clinical manifestation of the N544S mutation has a late onset and that the mutation does not have a pronounced effect on visual acuity, the mother may not experience a visual disturbance.

Several cases of double mutations associated with corneal dystrophies other than macular corneal dystrophy have been described previously (Table 2). However, no case of a double mutation of *TGFBI* causing an autosomal dominant form of corneal dystrophy has previously been reported. The presence of a homozygous Q118X mutation of *MISI* and a heterozygous P501T mutation of *TGFBI* in the same individual was described [16]. The Q118X mutation of *MISI* causes gelatinous drop-like corneal dystrophy (GDLD) with an autosomal recessive mode of inheritance. The P501T mutation of *TGFBI* causes LCD type IIIA [6]. The clinical manifestation in this patient resembled that of GDLD but not that of LCD type IIIA. A patient with a clinical diagnosis of GDLD and heterozygous Q118X and Y184C mutations of *MISI* has also been described [17]. No other case of the Y184C mutation in *MISI* has been presented, so it is not clear whether this mutation in the homozygous state can cause GDLD. A patient with a clinical diagnosis of GDLD was found to be heterozygous for both Q118X and L186P

Table 2. Previous reports of double mutations associated with corneal dystrophy.

Case	Amino acid mutation	Hetero- or homozygote	Gene	Mode of inheritance	Phenotype of single mutation	Phenotype of double mutation	Reference
1	Q118X	Homozygote	*M1S1*	AR	GDLD	GDLD	[16]
	P501T	Heterozygote	*TGFBI*	AD	LCD		
2	Q118X	Heterozygote	*M1S1*	AR	GDLD	GDLD	[17]
	Y184C	Heterozygote	*M1S1*	Not identified	Not identified		
3	Q118X	Heterozygote	*M1S1*	AR	GDLD	GDLD	[18]
	L186P	Heterozygote	*M1S1*	AR	GDLD		
4	A546D	Heterozygote	*TGFBI*	AD	Polymorphic corneal amyloidosis or LCD	LCD	[19,20]
	P551Q	Heterozygote	*TGFBI*	Not identified	Not identified		
5	R124L	Heterozygote	*TGFBI*	AD	GCD	GCD	[21]
	DeltaT125-DeltaE126	Heterozygote	*TGFBI*	Not identified	Not identified		
Present case	R124H	Heterozygote	*TGFBI*	AD	ACD	ACD+LCD	Present study
	N544S	Heterozygote	*TGFBI*	AD	LCD		

Abbreviations: ACD, Avellino corneal dystrophy; AD, autosomal dominant; AR, autosomal recessive; GCD, granular corneal dystrophy; GDLD, gelatinous droplike corneal dystrophy; LCD, lattice corneal dystrophy.

mutations of *M1S1* [18]. Patients with a clinical diagnosis of atypical LCD were found to be heterozygous for both A546D and P551Q mutations of *TGFBI* [19,20]. The A546D mutation of *TGFBI* causes polymorphic corneal amyloidosis [22] or atypical LCD [23] with an autosomal dominant mode of inheritance. There have been no other reports of the P551Q mutation of *TGFBI*, so it is not clear whether a heterozygous P551Q mutation causes corneal dystrophy. Finally, a patient with a clinical diagnosis of granular corneal dystrophy was found to be heterozygous for both R124L and ΔT125-ΔE126 mutations of *TGFBI* [21]. There have been no other reports of the ΔT125-ΔE126 mutation of *TGFBI*.

A few studies have addressed the penetrance of inherited corneal dystrophy. LCD type IIIA caused by the P501T mutation of *TGFBI* [16] and atypical granular corneal dystrophy caused by the D123H mutation of *TGFBI* [24] are thought to have a low penetrance. Non-penetrance of ACD has also been described [25]. The penetrance of corneal dystrophies caused by the R124H or N544S mutations of *TGFBI* remains unclear.

In all previously reported cases of double mutations, the clinical phenotype resembled that of one but not both of the associated corneal dystrophies. In the cases described in the present study, the phenotype associated with the double mutation is the summation of both corneal dystrophies. These cases thus indicate that R124H and N544S mutations of *TGFBI* independently determine clinical manifestation.

REFERENCES

1. Skonier J, Neubauer M, Madisen L, Bennett K, Plowman GD, Purchio AF. cDNA cloning and sequence analysis of beta ig-h3, a novel gene induced in a human adenocarcinoma cell line after treatment with transforming growth factor-beta. DNA Cell Biol 1992, 11 511-22 [PMID: 1388724]
2 Munier FL, Korvatska E, Djemai A, Le Paslier D, Zografos L, Pescia G, Schorderet DF. Kerato-epithelin mutations in four 5q31-linked corneal dystrophies. Nat Genet 1997; 15·247-51 [PMID: 9054935]
3. Munier FL, Frueh BE, Othenin-Girard P, Uffer S, Cousin P, Wang MX, Heon E, Black GC, Blasi MA, Balestrazzi E, Lorenz B, Escoto R, Barraquer R, Hoeltzenbein M, Gloor B, Fossarello M, Singh AD, Arsenijevic Y, Zografos L, Schorderet DF. BIGH3 mutation spectrum in corneal dystrophies. Invest Ophthalmol Vis Sci 2002; 43·949-54 [PMID: 11923233]
4. Kannabiran C, Klintworth GK TGFBI gene mutations in corneal dystrophies. Hum Mutat 2006; 27·615-25 [PMID· 16683255]
5. Endo S, Nguyen TH, Fujiki K, Hotta Y, Nakayasu K, Yamaguchi T, Ishida N, Kanai A. Leu518Pro mutation of the beta ig-h3 gene causes lattice corneal dystrophy type I. Am J Ophthalmol 1999; 128.104-6 [PMID: 10482106]
6. Yamamoto S, Okada M, Tsujikawa M, Shimomura Y, Nishida K, Inoue Y, Watanabe H, Maeda N, Kurahashi H, Kinoshita S, Nakamura Y, Tano Y. A kerato-epithelin (betaig-h3) mutation in lattice corneal dystrophy type IIIA. Am J Hum Genet 1998; 62.719-22 [PMID 9497262]
7. Fujiki K, Hotta Y, Nakayasu K, Yokoyama T, Takano T, Yamaguchi T, Kanai A. A new L527R mutation of the betaIGH3 gene in patients with lattice corneal dystrophy with deep stromal opacities. Hum Genet 1998, 103 286-9 [PMID. 9799082]
8 Mashima Y, Yamamoto S, Inoue Y, Yamada M, Konishi M, Watanabe H, Maeda N, Shimomura Y, Kinoshita S. Association of autosomal dominantly inherited corneal dystrophies with BIGH3 gene mutations in Japan. Am J Ophthalmol 2000, 130 516-7 [PMID: 11024425]
9. Dighiero P, Drunat S, Ellies P, D'Hermies F, Savoldelli M, Legeais JM, Renard G, Delpech M, Grateau G, Valleix S. A new mutation (A546T) of the betaig-h3 gene responsible for a French lattice corneal dystrophy type IIIA. Am J Ophthalmol 2000; 129·248-51 [PMID 10682981]
10. Kawashima M, Yamada M, Funayama T, Mashima Y. Six cases of late-onset lattice corneal dystrophy associated with gene mutations induced by the transforming growth factor-beta

Nippon Ganka Gakkai Zasshi 2005, 109 93-100 [PMID 15770959]

11 Mashima Y, Konishi M, Nakamura Y, Imamura Y, Yamada M, Ogata T, Kudoh J, Shimizu N Severe form of juvenile corneal stromal dystrophy with homozygous R124H mutation in the keratoepithelin gene in five Japanese patients Br J Ophthalmol 1998; 82 1280-4 [PMID 9924333]

12 Okada M, Yamamoto S, Watanabe H, Inoue Y, Tsujikawa M, Maeda N, Shimomura Y, Nishida K, Kinoshita S, Tano Y Granular corneal dystrophy with homozygous mutations in the kerato-epithelin gene Am J Ophthalmol 1998, 126 169-76 [PMID 9727509]

13. Okada M, Yamamoto S, Inoue Y, Watanabe H, Maeda N, Shimomura Y, Ishii Y, Tano Y. Severe corneal dystrophy phenotype caused by homozygous R124H keratoepithelin mutations Invest Ophthalmol Vis Sci 1998, 39·1947-53 [PMID 9727418]

14 Fujiki K, Hotta Y, Nakayasu K, Kanai A Homozygotic patient with betaig-h3 gene mutation in granular dystrophy Cornea 1998, 17 288-92. [PMID 9603385]

15. Inoue T, Watanabe H, Yamamoto S, Inoue Y, Okada M, Hori Y, Maeda N, Hayashi K, Shimomura Y, Tano Y. Different recurrence patterns after phototherapeutic keratectomy in the corneal dystrophy resulting from homozygous and heterozygous R124H BIG-H3 mutation Am J Ophthalmol 2001, 132 255-7 [PMID 11476689]

16 Ha NT, Fujiki K, Hotta Y, Nakayasu K, Kanai A Q118X mutation of M1S1 gene caused gelatinous drop-like corneal dystrophy the P501T of BIGH3 gene found in a family with gelatinous drop-like corneal dystrophy Am J Ophthalmol 2000, 130 119-20 [PMID. 11004271]

17 Tian X, Fujiki K, Li Q, Murakami A, Xie P, Kanai A, Wang W, Liu Z. Compound heterozygous mutations of M1S1 gene in gelatinous droplike corneal dystrophy Am J Ophthalmol 2004, 137·567-9. [PMID· 15013888]

18 Taniguchi Y, Tsujikawa M, Hibino S, Tsujikawa K, Tanaka T, Kiridoushi A, Tano Y. A novel missense mutation in a Japanese patient with gelatinous droplike corneal dystrophy Am J Ophthalmol 2005, 139 186-8 [PMID 15652848]

19 Klintworth GK, Bao W, Afshari NA Two mutations in the TGFBI (BIGH3) gene associated with lattice corneal dystrophy in an extensively studied family Invest Ophthalmol Vis Sci 2004, 45 1382-8. [PMID 15111592]

20 Aldave AJ, Gutmark JG, Yellore VS, Affeldt JA, Meallet MA, Udar N, Rao NA, Small KW, Klintworth GK Lattice corneal dystrophy associated with the Ala546Asp and Pro551Gln missense changes in the TGFBI gene Am J Ophthalmol 2004, 138:772-81 [PMID 15531312]

21 Dighiero P, Drunat S, D'Hermies F, Renard G, Delpech M, Valleix S A novel variant of granular corneal dystrophy caused by association of 2 mutations in the TGFBI gene-R124L and DeltaT125-DeltaE126 Arch Ophthalmol 2000, 118.814-8 [PMID. 10865320]

22 Eifrig DE Jr, Afshari NA. Buchanan HWt, Bowling BL, Klintworth GK Polymorphic corneal amyloidosis. a disorder due to a novel mutation in the transforming growth factor beta-induced (BIGH3) gene. Ophthalmology 2004, 111 1108-14 [PMID: 15177960]

23. Correa-Gomez V, Villalvazo-Cordero L, Zenteno JC. The TGFBI A546D mutation causes an atypical type of lattice corneal dystrophy Mol Vis 2007, 13 1695-700 [PMID 17893671]

24 Ha NT Cung le X, Chau HM, Thanh TK, Fujiki K, Murakami A, Kanai A A novel mutation of the TGFBI gene found in a Vietnamese family with atypical granular corneal dystrophy Jpn J Ophthalmol 2003; 47.246-8. [PMID· 12782158]

25 Kim JW, Kim HM, Song JS. Phenotypic non-penetrance in granular corneal dystrophy type II Graefes Arch Clin Exp Ophthalmol 2008; 246 1629-31 [PMID 18458933]

The print version of this article was created on 11 May 2009. This reflects all typographical corrections and errata to the article through that date. Details of any changes may be found in the online version of the article.

THE JOURNAL OF DERMATOLOGY

CASE REPORT

Epidermolysis bullosa nevus arising in a patient with Dowling–Meara type epidermolysis bullosa simplex with a novel K5 mutation

Hiroko SUGIYAMA-FUKAMATSU, Norihiro SUZUKI, Gen NAKANISHI, Keiji IWATSUKI

Department of Dermatology, Okayama University Graduate School of Medicine, Dentistry and Pharmaceutical Sciences, Okayama, Japan

ABSTRACT

We report herein a 4-year-old girl with Dowling–Meara type epidermolysis bullosa (EB) who presented with peculiar pigmented nevi. Blister formation had repeatedly occurred on the erythematous plaques in a circinate fashion since birth, and marked hyperkeratosis was observed on the palms and soles associated with nail deformity. Her mother and maternal grandmother also had similar symptoms. In addition to the blistering lesions, the patient had three large, asymmetrical, pigmented plaques with color variegation. Light and electron microscopic findings of the blistering lesions showed a subepidermal blister with intracytoplasmic granules in keratinocytes as well as degeneration of basal cells and aggregation of tonofilaments. The pigmented lesions revealed histopathological features of compound nevus without malignant changes. Gene analysis revealed an E478K (Glu to Lys) mutation in exon 5 of the *keratin 5* (*K5*) gene. These findings, together with clinical features, were consistent with those of Dowling–Meara type EB associated with so-called EB nevus.

Key words: Dowling-Meara type, epidermolysis bullosa, keratin 5 mutation, nevus.

INTRODUCTION

Patients with hereditary epidermolysis bullosa (EB) may present with a peculiar type of nevocellular nevi that usually form large, asymmetrical, irregular-shaped pigmented lesions, mimicking malignant melanoma.[1–3] Although both the clinical and dermoscopic findings are similar to those of malignant melanoma, the histopathological pictures and clinical courses are usually benign.[2–8] This type of nevi, therefore, has been called epidermolysis bullosa nevus.[3,8] We recently experienced a patient with familial Dowling–Meara type EB who presented with so-called EB nevus. We report herein our case, together with the clinicopathological findings, information regarding the responsible gene mutation and cytological profiles of the nevus cells.

CASE REPORT

A 4-year-old Japanese girl was referred to our hospital due to repetitive blistering since birth. The patient had been admitted to the neonatal intensive care unit at a nearby hospital during the postnatal period because of blistering on the trunk, extremities and oral cavity. At the age of 1 year, she presented with hyperkeratosis on the palms and soles without skin contracture. Her mother and maternal grandmother also had similar symptoms when young, but their symptoms became milder as they grew. Until the first visit to our hospital, she had been treated under a

Correspondence Keiji Iwatsuki, M.D., Ph.D., Department of Dermatology, Okayama University Graduate School of Medicine, Dentistry and Pharmaceutical Sciences, 2-5-1 Shikata-cho, Okayama 700-8558, Japan Email keijiiwa@cc.okayama-u.ac.jp
Received 12 September 2008, accepted 2 April 2009

diagnosis of hereditary EB, without confirmation of the clinical subtype and responsible gene mutation.

On physical examination, the patient presented with multiple bullae, erosions and erythematous plaques on the trunk and extremities (Fig. 1a,b). Fresh bullae and vesicles were observed in the periphery of the erythematous plaques in a circinate pattern. Keratoderma was found in palms and soles (Fig. 1c), and all the toes and fingernails were deformed (Fig. 1d). Her mother had one eroded lesion on the upper arm and dystrophic fingernails (Fig. 1d), and nail deformities on the fingers. In addition to these cutaneous manifestations, three asymmetric, irregularly-pigmented plaque lesions were observed on the chest, neck and upper arm (Fig. 2a,b). Erosions and scarring were also present in the pigmented lesions.

In order to determine the subtype of hereditary EB, we obtained a skin biopsy for light and electron microscopic observations, and a peripheral blood sample from the patient and mother under informed consent. Furthermore, a skin biopsy was obtained from the pigmented lesion to confirm the diagnosis.

The skin biopsy from the vesicle disclosed a subepidermal blister and the presence of intracytoplasmic granules in keratinocytes (Fig. 3a). Electron microscopic findings showed degeneration of basal cells as well as aggregation of tonofilaments in the keratinocytes (Fig. 3b). Based on the microscopic observations, together with the clinical features, we diagnosed the patient with Dowling–Meara type EB.

Using DNA samples extracted from the peripheral blood cells of the patient and her mother, keratin 5 (K5) genomic DNA was amplified with a polymerase chain reaction (PCR) as previously described,[9,10] and the PCR products were directly sequenced using an ABI373A automated DNA sequencer. The results demonstrated a G-to-A mutation in the exon 5, which caused a transition from Glu to Lys at the 478th amino acid (E478K) (Fig. 4).

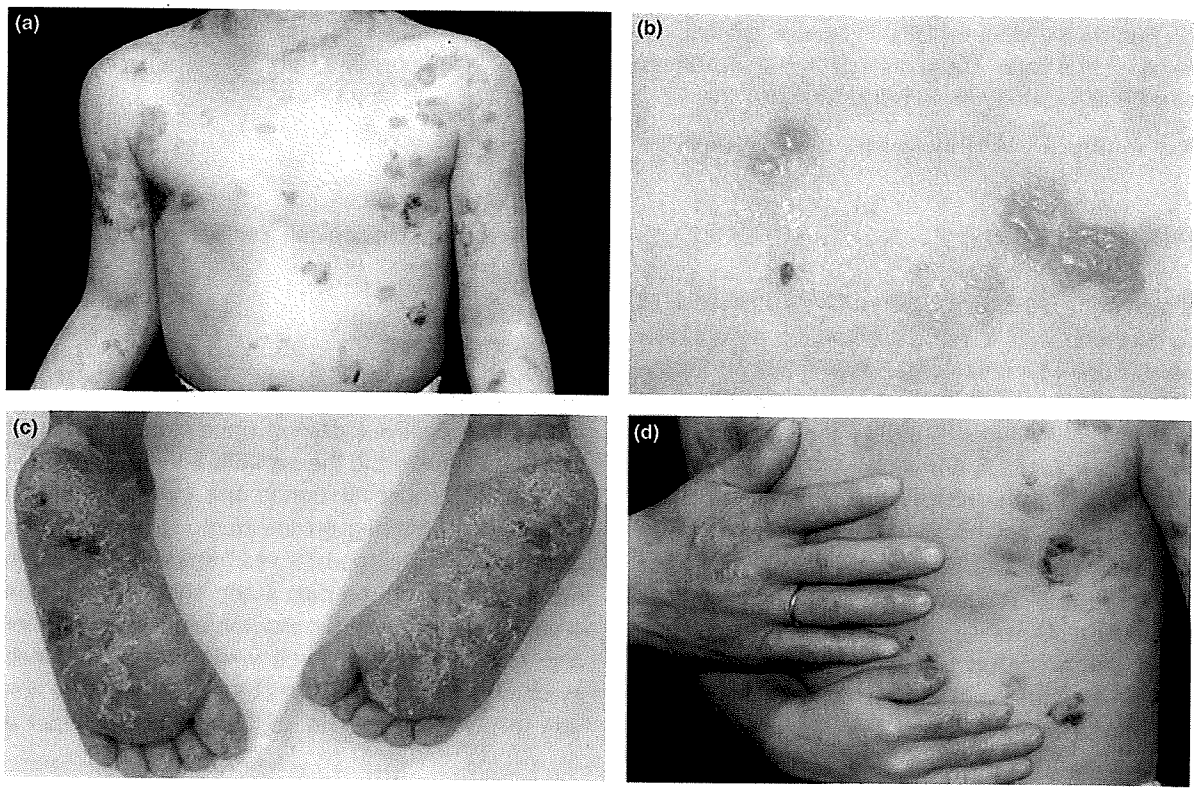

Figure 1. Fresh erythemic plaques with bullae and erosions on the trunk (a), herpetiform vesicles (b), keratoderma on the soles (c) and nail deformities on the fingers (d). The mother also has fingernail deformities and superficial scar formation on the dorsal surface of the hands (d).